

# Long-term stationarity of El Niño–Southern Oscillation teleconnections in southeastern Australia

Linden Ashcroft<sup>1,2</sup> · Joëlle Gergis<sup>1</sup> · David John Karoly<sup>1</sup>

Received: 11 February 2015 / Accepted: 29 June 2015 / Published online: 18 July 2015  
© Springer-Verlag Berlin Heidelberg 2015

**Abstract** The El Niño–Southern Oscillation (ENSO) phenomenon plays a large role in the modulation of Australian rainfall, particularly in the highly populated southeast. However, this influence is not stationary over time: weak ENSO teleconnections in Australia have been identified during 1920–1950, and palaeoclimate reconstructions indicate that a breakdown in global ENSO teleconnections may have also occurred in the early to mid-1800s. A lack of long-term instrumental data has prevented detailed examination of this intriguing earlier period. This study uses newly recovered instrumental rainfall observations to determine whether the weakening of ENSO teleconnections in the nineteenth century is apparent in eastern and southern southeastern Australia (SEA). Quantitative rainfall and rainday data from 1788 to 2012 are compared with three ENSO indices derived from palaeoclimate data. Statistical analysis suggests a weakening of the relationship between ENSO and SEA rainfall in the early nineteenth century data (~1835–1850), supporting results reported in previous global and regional studies based on palaeoclimate and documentary rainfall reconstructions. Possible causes of this weakening in teleconnection strength are then explored by examining a range of Southern Hemisphere circulation indices. The 1835–1850 period of low ENSO–SEA rainfall correlations appears to be characterised by a combination of reduced La Niña events and ENSO variance associated with a positive phase of the

Interdecadal Pacific Oscillation, with the possible influence of a predominately negative phase of the Southern Annular Mode. However, current temporal and geographical data limitations prevent definitive conclusions from being drawn. Despite these caveats, this study illustrates the considerable value of historical instrumental climate data in assessing long-term variations in climate mode teleconnections, particularly in the data-poor Southern Hemisphere.

**Keywords** Historical climatology · Palaeoclimatology · Southeastern Australia · Instrumental data · El Niño–Southern Oscillation · Teleconnections · Southern Hemisphere

## 1 Introduction

El Niño—Southern Oscillation (ENSO) is the leading influence of interannual global climate variability (Ropelewski and Halpert 1987; Allan et al. 1996). Broadly characterised by sea surface temperature and atmospheric pressure dipoles across the tropical Indo-Pacific region (McBride and Nicholls 1983; Risbey et al. 2009), ENSO influences temperature, rainfall and atmospheric pressure in many places around the world (Allan et al. 1996), either directly through tropical pressure variability or remotely through teleconnection patterns (Cai et al. 2011).

Australian climate is particularly sensitive to ENSO: El Niño events generally manifest as warm and dry conditions, while cool and wet conditions often prevail during La Niña events (McBride and Nicholls 1983; Allan et al. 1996; Risbey et al. 2009). This relationship is strongest in inland eastern Australia (McBride and Nicholls 1983), and is asymmetrical (Power et al. 2006), with the strength of La Niña events being more related to the size of positive

✉ Linden Ashcroft  
lindenclaire.ashcroft@urv.cat

<sup>1</sup> School of Earth Sciences and ARC Centre of Excellence for Climate System Science, University of Melbourne, Parkville 3010, VIC, Australia

<sup>2</sup> Centre for Climate Change, University Rovira i Virgili, 43500 Tortosa, Spain

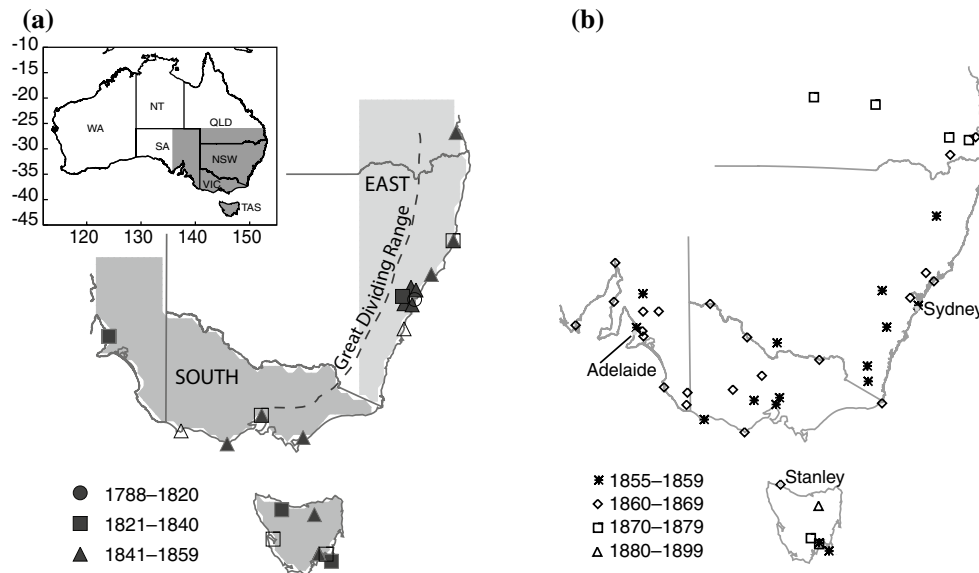


**Fig. 1** Location of SEA rainfall stations with data coverage from 1788 to 2012. **a** Rainfall observations available for the pre-1860 period, as identified by Ashcroft et al. (2014a). Symbols show the period in which observations began: 1788–1820 (circles), 1821–1840 (squares), 1841–1859 (triangles). Solid symbols indicate quantitative rainfall data availability, while open symbols indicate rain-day data only. The southern and eastern regions of SEA as defined

in this study are also shown. The SEA region and Australian states are shown in the Australian map (*inset*). **b** Rainfall stations with data for the 1860–2012 period, as outlined in Gergis and Ashcroft (2013). The symbols show the period in which rainfall records began at each station: pre-1860 (asterisk), 1860–1869 (diamond), 1870–1879 (squares) and 1880–1899 (triangles). Key locations and geographical features mentioned in the text are also marked

rainfall anomalies than the strength of El Niño events are associated with the magnitude of rainfall deficits.

The relationship between ENSO and the highly populated southeastern region of Australia (SEA, Fig. 1) is somewhat more complex, due to local topography and the influence of additional remote, large-scale atmospheric and oceanic circulation features (Risbey et al. 2009). Rainfall on the coastal region east of the Great Dividing Range is only weakly correlated with ENSO (Risbey et al. 2009; Timbal 2010), with coastal systems and zonal wind flow dominating rainfall variability (Rakich et al. 2008; Timbal 2010). Sea surface temperature variations in the tropical Indian Ocean exert an independent influence on SEA rainfall (e.g. Meyers et al. 2007; Ummenhofer et al. 2011), as do mid-latitude atmospheric pressure patterns such as the sub-tropical ridge (Timbal and Drosowsky 2013) and the Southern Annular Mode (Hendon et al. 2007). These features do not occur in isolation either, and interactions between them have been found to both enhance and reduce the ENSO influence in various subregions of SEA (e.g. Cai et al. 2011; Pepler et al. 2014).

ENSO's influence on Australian and global climate also exhibits multidecadal variability, hereafter referred to as low-frequency fluctuations (Power et al. 1999; Gallant et al. 2013). The 1920–1950 period is a well-known time of weakened ENSO teleconnections, with decreases in the influence of ENSO identified in many Australian and global

climate studies (e.g. Allan et al. 1996; Cole and Cook 1998; Power et al. 1999; Knippertz et al. 2003). Palaeoclimate and documentary reconstructions from ENSO-sensitive areas also indicate that the early 1800s were dominated by low ENSO activity and a weakening of regional and global ENSO teleconnections (e.g. Mann et al. 2000).

In fact, a rainfall reconstruction for SEA developed by Gergis et al. (2012) from palaeoclimate data suggests there was a marked breakdown in the SEA rainfall–ENSO relationship during the early to mid-1800s. Understanding these low-frequency variations in ENSO teleconnection strength is crucial for water management and agricultural planning in SEA (Meinke et al. 2005). However, high-quality instrumental rainfall observations used for Australian climate research are generally only available from the early twentieth century (Lavery et al. 1997; Alexander et al. 2010), hampering efforts to explore the stationarity of nineteenth century ENSO–Australian rainfall teleconnections (Power et al. 1998; Nicholls et al. 2006).

The dynamical mechanisms influencing decreases in the low-frequency variations of ENSO teleconnections, particularly in the SEA region, are still unclear (Power et al. 1998). One theory is that the Interdecadal Pacific Oscillation (IPO), a multidecadal ENSO-like SST pattern in the Pacific, modulates the intensity and influence of ENSO events, with negative IPO phases associated with a weakening in ENSO teleconnection strength (Power et al. 1999).

Stochastic changes in internal oceanic circulation, ENSO variance and periodicity, or a decoupling of the atmospheric and oceanic components of ENSO have also been identified as possible contributors (Kestin et al. 1998; Allan 2000). Cooler global temperatures due to volcanic eruptions or other external climate forcings have additionally been linked to the suppression of ENSO teleconnections (Reason et al. 1998; Mann et al. 2000), while some statistical analyses of global ENSO–rainfall correlations suggest that there may be no physical basis behind changes in teleconnection strength, and that low-frequency fluctuations are essentially random (van Oldenborgh and Burgers 2005; Wittenberg 2009).

In recent years, newly recovered instrumental data have allowed for the extension of homogenised monthly rainfall observations for SEA back to 1860 (Timbal and Fawcett 2012; Gergis and Ashcroft 2013; Ashcroft et al. 2014b). Further historical data recovery by Ashcroft et al. (2014a) provides additional instrumental data for regions of SEA as far back as European settlement in 1788. Combined with recently consolidated documentary rainfall data (Fenby and Gergis 2013), these historical datasets provide a new opportunity to explore SEA rainfall variability in the early to mid-nineteenth century.

The aim of this study is to determine whether the ENSO teleconnection breakdown reported elsewhere during the early to mid-nineteenth century (Mann et al. 2000) is present in the newly recovered rainfall observations for SEA. The historical instrumental data may provide verification of the palaeoclimate analysis of Gergis et al. (2012), broaden the analysis of long-term eastern SEA rainfall variability conducted by Gergis and Ashcroft (2013), and shed more light on the behaviour of ENSO during the 1800s.

The structure of this study is as follows. The historical data are described in Sects. 2 and 3, illustrating wet and dry periods in SEA during the period of continuous rainfall data availability. Stationarity in the ENSO–SEA rainfall relationship during 1788–2012 is then explored in Sect. 4 using a range of palaeoclimate ENSO reconstructions. Finally, in Sect. 5, the new historical dataset for SEA is used to investigate possible influences on ENSO–SEA rainfall teleconnection in the early to mid-nineteenth century.

## 2 Data

### 2.1 Instrumental and documentary data

Data for the pre-1860 period were extracted from the historical SEA dataset developed by Ashcroft et al. (2014a). This observational network includes newly recovered data from 21 rainfall and 27 rainday archival sources across SEA, and is the first instrumental dataset for the region to

extend to European settlement in 1788 (Fig. 1). The historical data have been examined for biases and inhomogeneities (Ashcroft et al. 2014a), and analysis shows that the rainfall records in particular are in good agreement with concurrent documentary SEA rainfall records (Gergis et al. 2012; Fenby and Gergis 2013; Ashcroft et al. 2014a).

Homogenised monthly rainfall data for 1860–2009 were taken from the observational network of 45 long-term SEA rainfall stations described in Gergis and Ashcroft (2013, Fig. 1b). To incorporate the wet period across Australia during 2010–2012 (e.g. Hendon et al. 2013) and account for limited data availability from the long-term rainfall stations post-1970 (Gergis and Ashcroft 2013), additional rainfall data were obtained from the Australian Bureau of Meteorology (BoM) interpolated Australian Water Availability Project (AWAP) dataset (Jones et al. 2009). Data from the  $0.05^\circ \times 0.05^\circ$  AWAP gridded product were extracted from the gridpoint closest to each of the 45 long-term rainfall stations. The mean difference between the instrumental and AWAP values was then calculated and added to the instrumental values. This step made minimal difference to the 1860–2009 instrumental rainfall data (the differences for both eastern and southern SEA normalised precipitation anomaly series were  $<0.04$ ), but was implemented to provide consistency between the two datasets.

Rainday counts from the SEA cities of Sydney and Adelaide (Fig. 1) were also used as local proxies for rainfall variability in eastern and southern SEA. Rainday counts from Ashcroft et al. (2014a) and the BoM observational network were combined for 1826–2012 for Sydney (BoM station number 066062) and 1839–2012 for Adelaide (BoM station numbers 023000 and 23090). Raindays from BoM were taken as days with more than 0.2 mm of rainfall to best match the seasonal cycle of raindays counts in the historical 1788–1860 data. Unfortunately no information on the threshold used for the historical rainday counts could be located (Ashcroft et al. 2014a).

The data were then separated into eastern and southern SEA regions (shown in Fig. 1) due to low data availability in the pre-1860 period and the differing climate features that are known to influence these subregions (Risbey et al. 2009; Timbal 2010). To compare relative rainfall variability across the full 1788–2012 time period, rainfall values were converted into normalised precipitation anomalies (NPA) relative to 1910–1950 values as described in Gergis and Ashcroft (2013). The 1860–2012 values were combined into SEA, eastern and southern SEA area-averages using Thiessen polygons (Thiessen 1911), while the 1788–1859 rainfall NPAs were arithmetically averaged due to the lower spatial data coverage available for analysis.

It should be noted that the rainfall and rainday data for eastern SEA are largely concentrated in the Sydney region before 1840, meaning that they may not capture the full

range of eastern SEA rainfall variability as defined in this study. An examination of the spatial correlations between twentieth century Sydney rainfall and SEA gridded rainfall data (Gergis and Ashcroft 2013), however, revealed that modern Sydney rainfall variability is significantly correlated with rainfall along the eastern NSW seaboard, with correlations decreasing sharply to the west of the Great Dividing Range (Timbal 2010). This coherence suggests that the pre-1840 eastern SEA data can be used to infer some rainfall variability in the broad region of eastern SEA marked in Fig. 1.

Documentary information on rainfall variability in SEA for 1788–1859 was taken from the SEA rainfall reconstruction of Fenby and Gergis (2013). This study analysed 12 documentary compilations of rainfall variability across SEA, building a comprehensive index of wet and dry years for the region. As discussed in Ashcroft et al. (2014a), the documentary chronology is in good agreement with instrumental rainfall data available for the pre-1860 period, and was used to represent rainfall variations when instrumental data were not available.

## 2.2 Circulation indices

Several palaeoclimate ENSO reconstructions were used to explore the stationarity of teleconnections in SEA over the 1788–2012 period. Gergis and Fowler's (2009) ENSO chronology (GF09), determined using 15 palaeoclimate and documentary records from ENSO sensitive regions, was used for analysis of discrete ENSO events. GF09 provides an annual assessment of the occurrence and strength of El Niño and La Niña events from 1525 to 2002.

The palaeoclimate records of ENSO variability developed by Li et al. (2013) and Emile-Geay et al. (2013) were also used to examine correlation changes in the ENSO–SEA rainfall relationship. The Li et al. (2013) reconstruction (Li13) combines 2222 tropical and sub-tropical tree-ring chronologies to create an annual reconstruction for November–January sea surface temperature (SST) variability in the Niño3.4 region (5°S–5°N, 170°W–120°W) over the 1301–2005 period. Emile-Geay et al. (2013, EG13) used two independent methods to combine tropical coral, tree-ring, ice-core and sediment records that displayed significant relationships with ENSO to reconstruct an estimate of SST variability in the Niño3.4 region, with most statistical skill identified for 1500–1995. The Pearson's correlation coefficient between the Li13 and EG13 reconstructions during the overlapping 1500–1995 period is 0.43, increasing to 0.63 for the 1788–1995 period of interest.

The SEA historical rainfall records and ENSO correlations were also compared to several palaeoclimate reconstructions of other Southern Hemisphere circulation features that influence SEA climate. Interdecadal Pacific

Oscillation (IPO) phases for the pre-instrumental period were determined from the McGregor et al. (2010) Unified ENSO Proxy index (UEP), which was developed by combining nine previously published ENSO reconstructions. The UEP has been smoothed with a 13-year Lanczos low-pass filter to capture the IPO signal (McGregor et al. 2010). Linsley et al. (2008)'s reconstruction of variations in the South Pacific Convergence Zone (SPCZ) was used as an additional index of IPO variability, as changes in the SPCZ are closely linked to variations in the IPO (Folland et al. 2002).

Finally, Southern Annular Mode (SAM) reconstructions developed by Abram et al. (2014) and Villalba et al. (2012) were used to represent SAM variability. Villalba et al. (2012) used the tree rings of over 3000 trees from Australia, New Zealand and South America to derive the hemispheric variability of the SAM during austral summer (December–February, DJF) from 1409 to 2006. The Abram et al. (2014) annual SAM reconstruction covering 1000–2007 was derived from ice cores taken from James Ross Island off the Northern Antarctic Peninsula and South American tree ring data. While the variations in the Abram et al. (2014) reconstruction are most closely linked to SAM behaviour in the Drake Passage region, their analysis indicates that the SAM in this area is highly correlated with the zonal SAM average on annual or longer timescales (Abram et al. 2014).

## 3 Eastern and southern SEA rainfall variability, 1832–2012

To examine long-term rainfall variability in eastern and southern SEA, Fig. 2 shows the 5-year moving averages of annual NPAs relative to 1910–1950. Prolonged wet and dry periods are also shown, defined following Ummenhofer et al. (2011): 5-year moving averages of NPAs were calculated and a period classified as wet or dry if it crossed a threshold of one standard deviation above or below zero for at least two consecutive 5-year means. The starting point of each wet and dry period was defined as the central year of the 5-year period when the moving average crossed the zero line before reaching the threshold. The end of each period was classified as the year when the moving average failed to reach the cut-off for more than 1 year.

According to this definition, prolonged wet periods occurred in eastern SEA during 1859–1873, 1889–1895, 1949–1955 and 1971–1977. Southern SEA experienced extended wet conditions during 1837–1839, 1849–1851, 1870–1874, 1888–1893, 1918–1919, 1951–1955, 1971–1977 and 1991–1994. Seasonal analysis (not shown) indicated that the twentieth century wet periods in eastern SEA in particular were dominated by above-average rainfall in

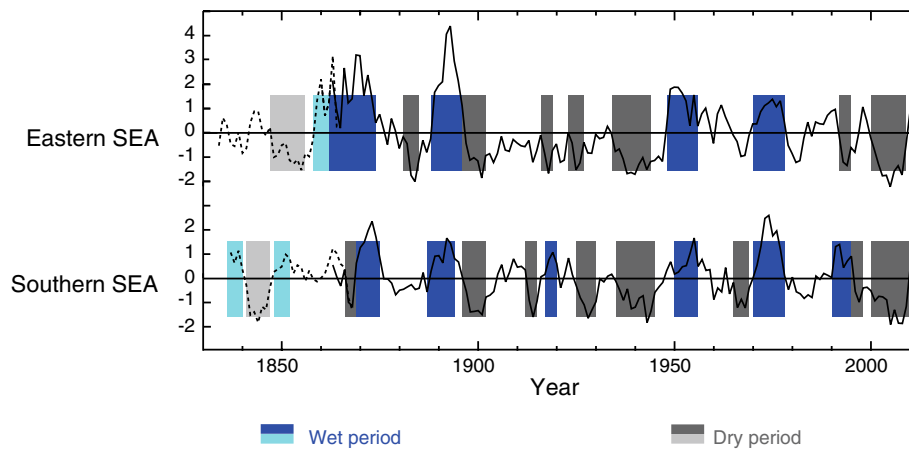


**Fig. 2** Five-year moving averages of annual rainfall in eastern SEA (*top*) and southern SEA (*bottom*), 1832–2012. Five-year running NPA means calculated using 1860–2012 data are shown in *solid lines*; means calculated using pre-1860 data are shown with *dashed lines*.

Five-year running means are plotted for the centre year of each 5-year period. Prolonged wet periods are indicated in *blue* (*light blue* for 1832–1859, *dark blue* for 1860–2012) and prolonged dry periods are shaded in *grey* (*light grey* for 1832–1859, *dark grey* for 1860–2012)

austral summer (December–February, DJF) and spring (September–November, SON), while pre-twentieth century wet periods were associated with above-average rainfall year-round or particularly wet austral autumns (March–May, MAM). This is an interesting result given the weak teleconnections between SEA rainfall and ENSO in austral autumn, and the significant drying that occurred during MAM in the 1997–2009 ‘Millennium Drought’ (Murphy and Timbal 2008; Verdon-Kidd and Kiem 2009).

Prolonged dry periods are identified in eastern SEA during 1848–1855, 1881–1883, 1897–1901, 1917–1918, 1924–1926, 1935–1943, 1993–1994 and 2001–2008. In southern SEA, extended dry spells occurred in 1842–1846, 1867–1868, 1897–1902, 1913–1914, 1926–1929, 1936–1944, 1966–1968, 1996–1997 and 2001–2009. Dry conditions experienced in southern SEA during the 1880s are also apparent, but are not extreme enough to classify as a prolonged drought according to the definition used in this study. The prolonged dry period in eastern SEA from 1848 to 1855 was largely associated with rainfall deficits in DJF and MAM (seasonal analysis not shown), while the southern SEA dry period during 1841–1845 was due to a decrease in rainfall in MAM and SON.

As described elsewhere (e.g. Nicholls 2010), the most recent 1997–2009 Millennium Drought in SEA was characterised by a dramatic reduction in MAM rainfall across both regions of SEA (seasonal analysis not shown). The prolonged dry period corresponding to the World War II drought (~1935–1945) was associated with a decrease in rainfall during all seasons and both subregions of SEA, while the Federation Drought (~1898–1904) was dominated by a decrease in rainfall during June–August (JJA) and SON over southern SEA (Verdon-Kidd and Kiem

2009) and during DJF and SON in eastern SEA. The data presented here are also in good agreement with other studies comparing the three major SEA droughts since the 1890s (Trewin and Fawcett 2009; Ummenhofer et al. 2009; Verdon-Kidd and Kiem 2009), which found that the recent 1997–2009 drought was the most severe in southern SEA, and the World War II drought and Millennium droughts were similar in duration.

Extending the rainfall record also provides some new information about nineteenth century SEA subregional climate variability (Gergis and Ashcroft 2013; Ashcroft et al. 2014a). The eastern SEA drought experienced during 1848–1855 appears to be as long as the World War II drought experienced in the subregion, although the negative rainfall anomalies during 1848–1855 were not as extreme in magnitude. It is interesting to note that southern SEA experienced a prolonged wet period during this time, in contrast to the World War II drought, which was dry across both eastern and southern SEA.

## 4 SEA–ENSO teleconnection stationarity, 1788–2012

### 4.1 Discrete ENSO event analysis

Next, the long-term stationarity of the ENSO–SEA rainfall relationship is examined using comparisons of discrete ENSO events. The focus here is on the relatively unexamined 1788–1870 period, complementing the palaeoclimate studies of nineteenth century ENSO teleconnection stationarity (Mann et al. 2000; Gergis et al. 2012) and extending the SEA-wide 1871–2009 analysis of Ashcroft et al. (2014b).

**Table 1** Eastern SEA wet and dry years compared to the Gergis and Fowler (2009) ENSO chronology (GF09) for the years with instrumental data available, 1788–1870

	El Niño	Neutral	La Niña
Dry rainday	1832, 1837, 1845, 1851, 1857	1834, 1835, 1838, 1841, 1853	(1823), 1849
Normal rainday	(1790, 1791, 1803), 1828, 1836, 1843, 1847, 1852, 1855, 1856	(1821), 1826, 1827, 1833, 1854	(1788, 1789), 1840
Wet rainday	1831, 1844	1829, 1830	(1804), 1839, 1842, 1846, 1849, 1850
Dry rain	1832, 1837, 1845, 1851, 1852, 1865	1834, 1838, 1854	(1822), 1848, 1849
Normal rain	1843, 1855, 1857, 1864	1835, 1853, 1858	1842, 1846, 1861
Wet rain	1836, 1844, 1847, 1856, 1863, 1866	(1821), 1833, 1841, 1868	1840, 1850, 1859, 1860, 1862, 1867, 1869, 1870

Wet and dry years are classified using rainday counts (top three rows) and rainfall amounts (bottom three rows). Years before 1826, when continuous observations begin, are printed in brackets. Wet and dry years are defined over May–April, and compared to the following calendar year of GF09 to align the period of greatest ENSO influence over Australia with the peak biological signal of the palaeoclimate ENSO reconstruction

**Table 2** As for Table 1, but for southern SEA

	El Niño	Neutral	La Niña
Dry rainday	1857	1841, 1854	1840, 1850
Normal rainday	1847	1838, 1853	1839, 1842, 1846, 1849
Wet rainday	1837, 1843, 1844, 1845, 1852, 1855, 1856	1833, 1841, 1868	1848
Dry rain	1843, 1844, 1847, 1864, 1865	1835, 1841, 1854, 1868	1850
Normal rain	1845, 1855, 1856, 1857, 1866	1838	1840, 1842, 1846, 1859, 1860, 1861, 1869
Wet rain	1836, 1837, 1851, 1852, 1863	1853, 1858	1848, 1849, 1862, 1867, 1870

Tables 1 and 2 compare wet and dry years in eastern and southern SEA with the discrete GF09 ENSO event chronology from 1788 to 1870. The wet and dry years refer to a May–April year, corresponding with the peak biological ENSO signal in the GF09 reconstruction (Gergis and Fowler 2009). The ENSO reconstruction values are compared to the following years of rainfall i.e. the ENSO value for 1888 is compared with the rainfall values for May 1888 to April 1889. Wet and dry years are defined as years with NPAs half a standard deviation above and below the 1910–1950 mean respectively, dividing the rainfall data into rough terciles following Ashcroft et al. (2014a). The standard deviation for the pre-1871 period was determined using the available 1788–1860 anomalies, rather than 1910–1950, to account for higher variance in the arithmetically averaged pre-1860 data.

The GF09–SEA rainfall comparison reveals generally weak to moderate relationships between GF09 and SEA rainfall variability over the periods of available instrumental data from 1788 to 1870. The rainfall data and rainday counts for eastern SEA show an approximation of the general ENSO signal (Risbey et al. 2009): more years with a low rainday count are associated with El Niño events than La Niña conditions, and years of above-average rainfall correspond more to La Niña years than El Niño years. However, these relationships are insignificant ( $p > 0.05$ )

using the Fisher–Freeman–Halton Exact Test for independence of a  $3 \times 3$  contingency table distribution (Freeman and Halton 1951). Interestingly, the dry years of 1848–1855 occurred at a similar time as protracted La Niña conditions (Allan and D’Arrigo 1999; Gergis and Fowler 2009), which are usually associated with above-average rainfall.

The southern SEA region shows an unexpected relationship between ENSO and rainfall for 1835–1870. While these distributions are not significant either, the general agreement between El Niño/Dry and La Niña/Wet is not apparent. In particular, the rainday counts show that seven out of 11 wet years between 1837 and 1857 (when rainday data are available) occurred during El Niño conditions. This reversed relationship is not as clear in the rainfall comparison, with dry conditions in the mid-1840s occurring at the same time as a protracted El Niño state (Gergis and Fowler 2009). Overall, El Niño events are associated with the same number of wet years as dry years in eastern SEA. Three of the seven El Niño events that are associated with a wet year in southern SEA were recorded as weak in GF09 (Gergis and Fowler 2009) which may explain this, but even if the weak ENSO events are removed from the comparison, no significant agreement emerges between southern SEA rainfall and ENSO over 1835–1870.

The 1788–1825 period is only represented by three isolated rainfall and rainday records in eastern SEA, shown

**Table 3** Eastern SEA wet and dry years from the Fenby and Gergis (2013) documentary rainfall chronology compared to the Gergis and Fowler (2009) ENSO chronology (GF09), 1788–1840

	El Niño	Neutral	La Niña
Dry	1790, 1791, 1798, 1802, 1803, 1811, 1813, 1814, 1815, 1828, 1837	1826, 1827, 1835, 1838	1809, 1810, 1824
Normal	1792, 1806, 1823, 1832	1795, 1799, 1817, 1820, 1821, 1825, 1833, 1834	1789, 1794, 1800, 1801, 1807, 1812, 1818, 1819, 1822
Wet	1793, 1797, 1805, 1816, 1831, 1836	1829, 1830	1788, 1796, 1804, 1808, 1839, 1840

Wet and dry years are defined over May–April, and compared to the following calendar year of GF09

**Table 4** Distribution of years (in rounded percentages) in each of the nine possible combinations of El Niño, neutral and La Niña phases with wet, normal and dry conditions, comparing May–April wet and dry years in eastern and southern SEA with GF09

	El Niño			Neutral			La Niña		
	All	RD	Rain	All	RD	Rain	All	RD	Rain
Eastern SEA									
Dry	<b>19</b>	<b>15</b>	<b>16</b>	3	<b>15</b>	8	5	3	5
Normal	<b>21</b>	<b>21</b>	<b>11</b>	8	12	8	9	9	8
Wet	11	6	16	2	6	8	<b>21</b>	<b>15</b>	<b>21</b>
Southern SEA									
Dry	<b>13</b>	5	<b>14</b>	5	<b>10</b>	11	5	<b>10</b>	3
Normal	<b>27</b>	5	14	5	10	3	17	<b>19</b>	<b>20</b>
Wet	12	<b>33</b>	<b>14</b>	4	5	6	<b>14</b>	5	<b>14</b>

Distributions are shown for 1871–2002 rainfall data (131 years, all), as well as rainday and rainfall classifications over the period of data availability: 1826–1857 for eastern SEA and 1837–1857 for southern SEA rainday data (RD), 1832–1870 for eastern SEA and 1835–1870 for southern SEA (rain). The highest percentage for each ENSO phase in each of the three possible rainfall categories are bold.

in brackets in Table 1. To provide a comprehensive analysis of ENSO–SEA rainfall co-variability since European settlement in 1788, Table 3 compares GF09 with the wet and dry years identified for eastern NSW from documentary sources by Fenby and Gergis (2013) for 1788–1840. Unfortunately the limits of colonial Australian settlement mean that there are not enough instrumental or documentary records to extend the analysis to southern SEA.

The documentary record for eastern SEA generally supports the findings of the instrumental data, showing weak to moderate ENSO–SEA rainfall teleconnections over the 1788–1840 period ( $p = 0.06$  using the Fisher–Freeman–Halton Exact Test). The most extreme ENSO event within the 1806–1820 period with no instrumental data is a protracted El Niño event during 1814–1817 (Gergis and Fowler 2009), which was associated with prolonged drought in the documentary record (Fenby and Gergis 2013). There also appears to be a number of La Niña events that were associated with normal, rather than wet, rainfall conditions in eastern SEA in the early 1800s. This may be due to the difficulties in determining wet years using documentary data (Brázdil et al. 2010; Fenby and Gergis 2013) and the enhanced role of local orographic features and

coastal systems on rainfall along Australia’s eastern seaboard (Speer et al. 2010).

When ENSO–SEA rainfall relationships over 1826–1870 (the period of continuous rainday data for eastern SEA) are compared to the long-term agreement between GF09 and rainfall over 1871–2002, the pre-1870 period stands out as one of weak ENSO teleconnections across southern SEA. Table 4 provides a visual comparison and shows the percentage of years in eastern and southern SEA that fall into each of the nine possible combinations of wet, dry and normal conditions with El Niño, neutral and La Niña phases for 1871–2002 and the pre-1871 period. ENSO phases are determined by the GF09 chronology. The ENSO phase that is associated with the most wet, normal and dry years in each period is highlighted.

The top left and bottom right boxes for each rainfall dataset are expected to be highlighted if the traditional ENSO–SEA rainfall relationship is present. The 1871–2002 period indeed shows a significant relationship between ENSO and SEA rainfall, with wet conditions occurring more frequently during La Niña events, and dry years more common during El Niño events ( $p < 0.05$ ). The eastern SEA data shows a similar pattern for 1825–1870,

both in rainfall data and rainy day counts, although the distribution is not statistically significant.

For the southern SEA region, this pattern is not as clear. No significant relationship between ENSO and SEA rainfall is apparent, and the rainy day counts indicate that wet years were more prevalent during El Niño years over 1837–1857, with 7 years (or 33 %) falling into this category. This compares to only 12 % over the 1871–2002 period. The percentage of wet years defined using rainfall data that occurred during La Niña years (14 %) during 1835–1870 is the same percentage that occurred during El Niño conditions. This is actually not a large deviation from the 1871–2002 distribution, where 14 % of wet years occurred during La Niña conditions and 12 % of wet years coincided with El Niño conditions. Although this discrete event analysis alone does not indicate a significant change in ENSO influence, it does suggest low agreement between ENSO conditions and southern SEA rainy day data during 1835–1870.

#### 4.2 Correlations between SEA rainfall and continuous ENSO reconstructions

Discrete event analyses between the GF09 ENSO chronology and the 1788–1870 SEA rainfall and rainy day data are valuable for the analysis of individual ENSO events and their societal impacts, but cannot provide adequate insight into the question of long-term stationarity in ENSO teleconnections. Another way to examine the relationship between ENSO and SEA climate is to evaluate correlations between SEA rainfall and continuous ENSO reconstructions, rather than discrete chronologies of ENSO events such as GF09.

To compare changes in the stationarity of ENSO teleconnections over the post-1832 period when rainfall data are available (post-1835 for southern SEA), Fig. 3 displays the 21-year moving correlations between annual (May–April) NPA for eastern and southern SEA and two ENSO reconstructions Li13 and EG13. ENSO reconstruction values are again compared to the following May–April rainfall and rainy day value. Periods of significant correlations are determined using the block bootstrapping method (Zwiers et al. 2011), to account for autocorrelation in the rainfall and ENSO series. An ensemble of 2000 synthetic 21-year blocks was created from random 3-year periods of each data series, and correlations calculated between each synthetic block. Significance levels are taken at the 2.5th and 97.5th percentiles of the resulting correlation probability distribution function.

The moving correlations reveal high variability in ENSO teleconnections over 1832–2005. Eastern SEA rainfall shows the weakened correlations with both ENSO reconstructions during the 1930s–1940s [previously identified by Kestin et al. (1998) and Allan et al. (1996), among

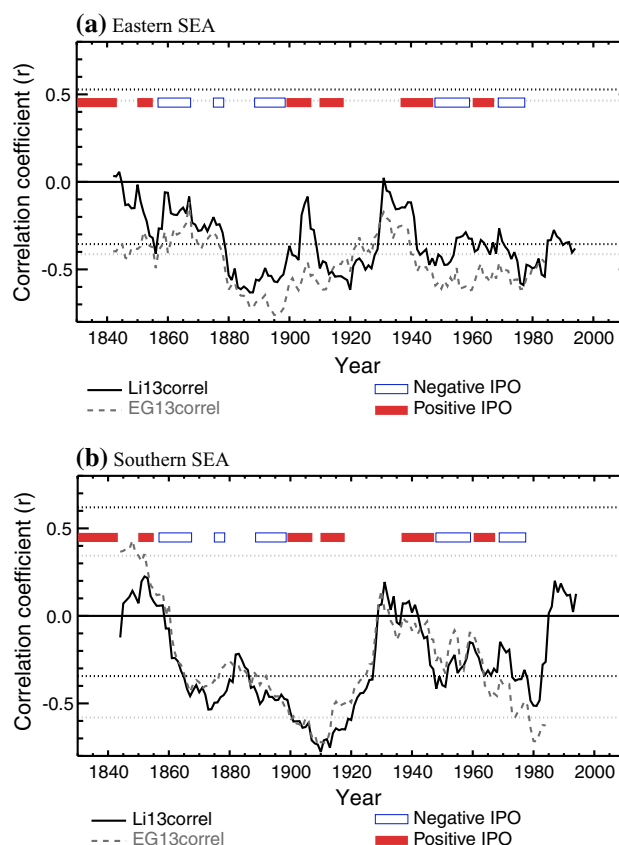


**Fig. 3** 21-year moving correlations between **a** eastern SEA rainfall and **b** southern SEA rainfall and Li13 (solid line) and EG13 (dashed line). Correlations are plotted on the centre year for each 21-year period. Variations in the IPO, calculated from McGregor et al. (2010)'s Unified ENSO proxy are also plotted. Correlations that are above or below the black dotted lines (Li13 correlations with eastern and southern NPA) and grey dotted lines (EG13 correlations with eastern and southern NPA) are statistically significant (significance levels determined using block bootstrapping)

others] and 1860s–1870s, with additional weak correlations between Li13 and eastern SEA rainfall during the early 1900s and the 1830s–1840s. Strong correlations between Li13, EG13 and eastern SEA rainfall occurs during the intervening periods, particularly during 1880–1900, which was also identified in the SEA-wide seasonal teleconnection analysis of Ashcroft et al. (2014b). The eastern SEA rainfall–EG13 correlations are slightly stronger than the eastern SEA rainfall–Li13 correlations, but the multidecadal variations are very similar for both reconstructions.

The correlations between Li13, EG13 and southern SEA rainfall are also in good agreement. Decreased correlations with ENSO are observed around 1930–1950, at the turn of the twentieth century and during the 1830s and 1840s, while strong correlations are observed during 1910–1920 and the 1970s (Allan et al. 1996). The ENSO–southern SEA rainfall correlations during the 1840s in particular



display a weakening and even a dramatic reversal towards positive correlations in the earliest part of the record, supporting the discrete event analysis reported earlier. The southern SEA–Li13 correlations also show a weakening in the most recent period (1985–2005), which is not present in the eastern correlations.

The results of these moving correlations in conjunction with the discrete ENSO event analysis suggest the historical instrumental data for SEA seems to indicate a weakening of ENSO teleconnections across the region during the early 1800s, similar to the well-known reduction of ENSO teleconnections during 1920–1950. In particular the data from southern SEA show a statistically significant reversal in the correlations between rainfall and ENSO. This finding is in general agreement with the Gergis et al. (2012) multiproxy palaeoclimate reconstruction of SEA rainfall, which found a complete breakdown between ENSO and their rainfall reconstruction during 1793–1840. Gergis et al. (2012) also identified a weakening or reversal in the relationship with ENSO and individual proxies used in their reconstruction, a finding supported by separate studies of single regional proxies [e.g. Fowler et al. (2012) for New Zealand tree-ring data and Lough (2007) for coral data from the Great Barrier Reef].

The results from the SEA historical instrumental data additionally agree with other studies of global nineteenth century ENSO variability. Mann et al. (2000) identified 1801–1850 as a period of dramatic global departure from standard ENSO teleconnections in their multiproxy analysis of ENSO back to 1650, while D'Arrigo (2005a, b) found a decrease in ENSO variability and associated teleconnections across the Northern Pacific during the mid-1800s. Conversely, other studies have found that this period was not associated with any unusual ENSO teleconnection behaviour. For example Nash and Endfield (2002, 2008) and Nash and Grab (2010) found largely consistent relationships between ENSO and nineteenth century southern African rainfall derived from documentary data, although they did note some exceptions during 1820–1840. Adamson and Nash (2014) found a peak in correlation between the western Indian monsoon and ENSO during 1835–1845.

Given these differences and the number of large-scale circulation features that influence SEA rainfall, it is worth exploring the different factors that could have affected the ENSO–SEA rainfall teleconnections during the nineteenth century. It may be that the results identified in this study are due to additional local influences, rather than global changes in ENSO behaviour. The spatial limitations and uncertain quality of the historical data must also be seriously considered as a potential variable that would confound the results. The following section provides a preliminary discussion of possible factors that may have contributed to the observed decrease in the ENSO

teleconnection identified over southern SEA during the early nineteenth century.

## 5 Possible influences on nineteenth century southeastern Australian rainfall–ENSO teleconnection variability

### 5.1 Historical rainfall data quality

The first possibility could be that the low ENSO–SEA rainfall correlations described in Sect. 4 are due to poor quality and spatial coverage of the historical rainfall observations. Although the historical observations have been rigorously examined for inhomogeneities and errors, they were not taken using modern standards, and limited metadata are available (Ashcroft et al. 2014a). The observations in the pre-1870 period are primarily from coastal regions (Ashcroft et al. 2014a, b) as well, where ENSO's influence on Australian rainfall is weaker (Risbey et al. 2009). As more stations data are introduced to the record, the correlations could artificially increase. The reliability of the ENSO reconstructions may also be questioned, although similar results were obtained using three independent records, which have all been rigorously checked against modern instrumental indices (Gergis and Fowler 2009; Emile-Geay et al. 2013; Li et al. 2013).

To test the influence of a smaller rainfall dataset on ENSO–SEA rainfall correlations, 21-year moving correlations were calculated between Li13, EG13 and long-term rainfall records from three SEA locations with the earliest rainfall data: Sydney, Adelaide, and western Tasmania. Rainfall data from the Stanley Post Office (BoM station number 91094) for 1883–1976 were used to represent rainfall variations near Hampshire Hills in northwestern Tasmania, where the earliest rainfall observations for southern SEA are available (Ashcroft et al. 2014a). Rainfall observations and rainy day counts from Adelaide (BoM station numbers 23000 and 23070) were used as an additional representation of southern SEA rainfall variability as they extend to 1839. Rainfall and rainy day data for Sydney from both pre-1860 and post-1860 datasets were combined to produce an annual record that covers 1832–2012 (Gergis and Ashcroft 2013).

Figure 4 compares the 21-year moving correlations between Li13, EG13 and annual (May–April) rainfall from Sydney, Adelaide, Stanley, and eastern and southern SEA. If the low ENSO–SEA rainfall correlations identified during the 1830s and 1840s are due to the limited number of rainfall observations alone, then moving correlations between the ENSO proxy records and single station rainfall would be expected to show consistently lower correlations than the regional rainfall values. Using rainfall and rainy day

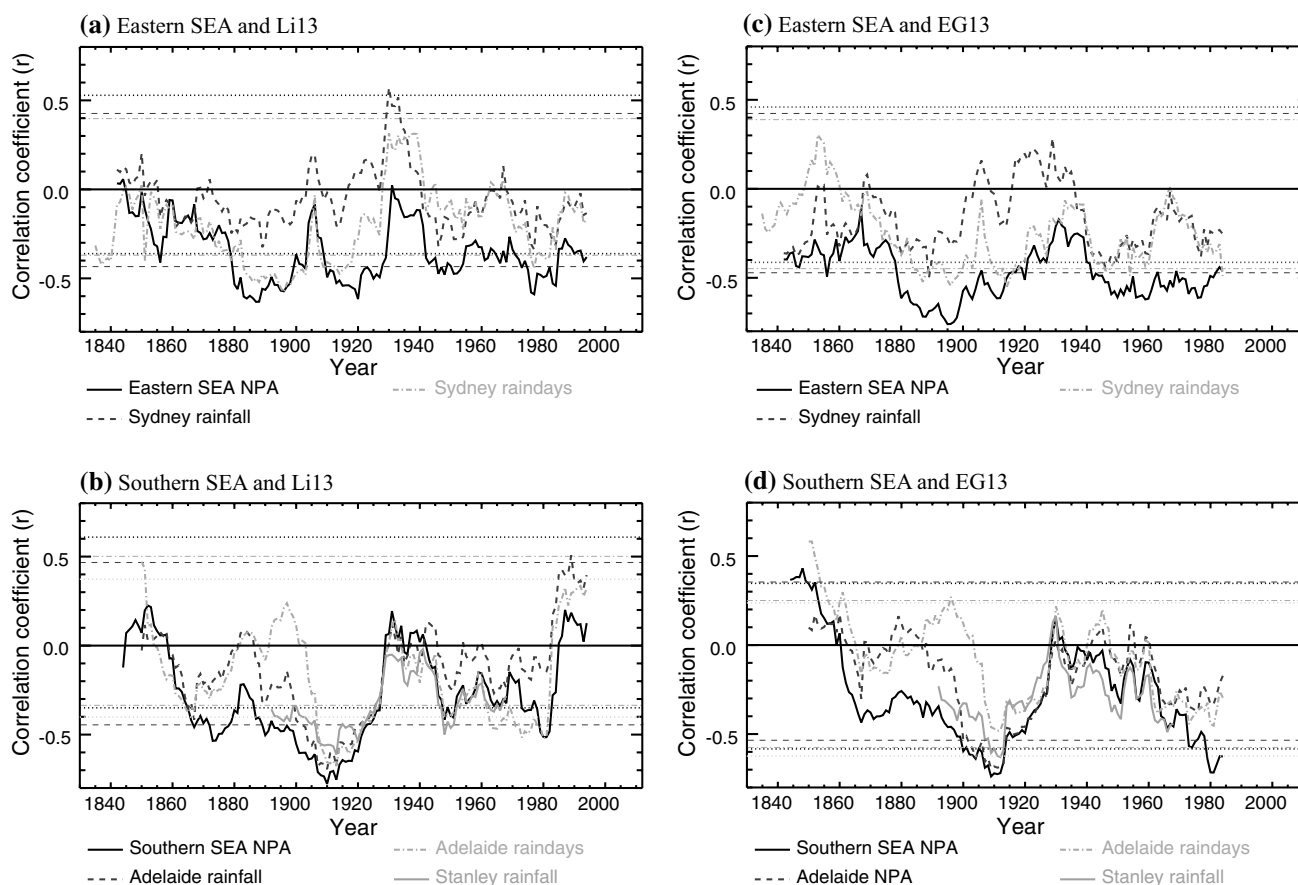


**Fig. 4** **a** 21-year moving correlations between the Li13 ENSO reconstruction and annual (May–April) rainfall for eastern SEA rainfall (solid black line) and Sydney (dashed black line), 1832–2005, as well as Sydney rainday counts (dashed grey line), 1826–2005. **b** as **a**, but for southern SEA, 1835–2005 (solid black line), Adelaide rainfall, 1839–2005 (black dashed line) and Stanley, western Tasmania, 1883–1976 (dashed grey line). **c** and **d** as **a** and **b** but for EG13. Correlations values are plotted against the central year of each 21-year

data from individual stations also provides further verification of the time-varying ENSO relationships observed in Fig. 3.

The correlations between Sydney rainfall and raindays and the ENSO reconstructions in Fig. 4 are similar to the correlations obtained using data from the broader eastern SEA rainfall region, although the Sydney correlations are generally lower. There is good agreement between the eastern SEA and Sydney correlations before the 1860s, but this is because the majority of the eastern SEA rainfall data comes from the Sydney region (Ashcroft et al. 2014a). Therefore, it could be that the weak rainfall–ENSO relationship in eastern SEA before about 1840 may be due to lower correlations between ENSO and rainfall in Sydney, compared to the wider SEA region. However, the relative fluctuations in the teleconnection strength are similar using both the eastern SEA and Sydney rainfall series: maximum

period. Correlations that are above or below the black dotted lines (Li13 and EG13 correlations with eastern and southern NPA), thin black dashed lines (Li13 and EG13 correlations with Sydney and Adelaide rainfall), thin grey dashed lines (Li13 and EG13 correlations with Sydney and Adelaide raindays) and grey dotted lines (Li13 and EG13 correlations with Stanley rainfall) are statistically significant (significance levels determined using block bootstrapping)

correlations are recorded during 1870–1890, and weaker correlations are observed around 1920–1950. This suggests that although the magnitude of the ENSO–Sydney rainfall relationship is somewhat weaker than that observed for the whole eastern SEA region, it displays similar low-frequency variability.

Comparing the correlations between Li13, EG13, southern SEA rainfall, Adelaide and Stanley rainfall also yields similar temporal variations between each rainfall series. All three moving correlation curves show the same fluctuations in teleconnection strength over time, although the rainfall records from Adelaide produce somewhat smaller absolute correlations than the southern SEA regional average, particularly during 1860–1900. It is encouraging to see that the ENSO–southern SEA correlations and ENSO–Stanley rainfall correlations display similar variability during the overlapping 1883–1976 period. This suggests

**Table 5** Correlations between ENSO and eastern and southern SEA rainfall variations during positive and negative phases of the IPO

	Linsley08		McGregor10	
	IPO+	IPO−	IPO+	IPO−
<b>Li13</b>				
Eastern SEA	−0.11 (43)	<b>−0.55</b> (38)	−0.14 (42)	<b>−0.58</b> (38)
Southern SEA	0.03 (41)	<b>−0.58</b> (38)	<b>−0.32</b> (40)	<b>−0.48</b> (36)
<b>EG13</b>				
Eastern SEA	<b>−0.42</b> (43)	<b>−0.52</b> (32)	<b>−0.39</b> (42)	<b>−0.62</b> (38)
Southern SEA	−0.19 (41)	<b>−0.53</b> (32)	<b>−0.35</b> (40)	<b>−0.49</b> (36)

ENSO variations are determined using the Li et al. (2013, Li13) and Emile-Geay et al. (2013, EG13) reconstructions, while the IPO is defined by the IPO reconstructions of Linsley et al. (2008, Linsley08) and McGregor et al. (2010, McGregor10). Positive IPO phases are classified as years with values above the 75th percentile, while negative IPO phases are classed as years with reconstruction values below the 25th percentile. The number of years within each category is given in brackets. Statistically significant correlations ( $p$  value  $<0.05$ , significant using the Student's two-tailed  $t$  test) are marked in bold

that the weak ENSO–southern SEA rainfall correlations during 1835–1840 when rainfall observations were only available from northwestern Tasmania may indeed represent a more region-wide decrease in ENSO teleconnection strength, although further analysis is required to confirm this inference.

The results for eastern and southern SEA indicate that the limited spatial distribution of historical rainfall data and the quality of the rainday observations may have caused some of the decrease in ENSO–SEA rainfall correlations during 1830–1850. These limitations are an unavoidable component of any historical climatology study (Brázdil et al. 2010), particularly in the Southern Hemisphere where there are fewer data sources for comparison. However, taking these limitations into account, there still appears to have been some variation in ENSO teleconnection strength in the early part of the nineteenth century in areas of SEA.

## 5.2 Multidecadal ENSO variability

If poor data coverage and reliability cannot completely explain the fluctuations in correlations between ENSO and eastern and southern SEA rainfall, then perhaps they are due to low-frequency variations in ENSO itself. There is palaeoclimatic evidence that the Interdecadal Pacific Oscillation (IPO)—effectively a measure of the low-frequency variability of ENSO (Power et al. 2006)—was in a positive phase from the 1820s to the 1850s (Verdon and Franks 2006), while both instrumental and palaeoclimate data show predominately positive conditions during the low teleconnection period of 1910–1940 (Power et al. 1999).

El Niño events are more prevalent during positive IPO phases (Power et al. 2006), and positive IPO conditions have also been associated with a decrease in ENSO variance (Arblaster et al. 2002), which can reduce the remote impact of ENSO events outside the tropical region (Torrence and Webster 1999; Allan 2000; Li et al. 2013). GF09 and Li13 do in fact report more El Niño events than La Niñas during the 1830s and 1840s, as well as a reduction in ENSO variance and the occurrence of extreme ENSO events. Conversely, EG13 suggests a similar number of El Niño and La Niña events occurred during this time.

Correlations between Li13, EG13 and eastern and southern SEA rainfall during positive and negative phases of the IPO determined by Linsley et al. (2008) and McGregor et al. (2010) are shown in Table 5. To capture the majority of IPO phases, positive IPO conditions were defined as years with a value above the 75th percentiles from each reconstruction, while negative IPO phases were classed as years with reconstruction values below the 25th percentiles. The results remained essentially unchanged if a more or less stringent threshold was used. The comparison reveals higher correlations between ENSO and SEA rainfall during negative IPO phases, particularly when using the Linsley et al. (2008) reconstruction. Directly comparing the IPO phases with moving correlations in Fig. 3 also suggests that the periods of low ENSO teleconnection strength are associated with positive IPO phases.

A tendency towards more El Niño events than La Niña events during the 1830s and 1840s may explain the low correlations between SEA rainfall and ENSO described here. As discussed by Power et al. (2006), La Niña events are more linearly associated with positive rainfall anomalies across Australia than El Niño events are associated with negative rainfall anomalies. This asymmetric relationship is expressed as weak correlations during El Niño dominant periods (positive IPO phases), and high correlations during La Niña dominant periods (negative IPO phases).

The coincident reduction in ENSO variance, due to internal or external forcings that are beyond the scope of the current study (Mann et al. 2000), also means that there were no extreme ENSO events to exert a significant influence on eastern and southern SEA climate variability. Mann et al. (2000) has previously associated the unusual global teleconnections in the early nineteenth century with a breakdown in interannual ENSO variability, while Li et al. (2013) identified low ENSO teleconnections across the Pacific region during times of low ENSO variance over the past 700 years.

## 5.3 Indian Ocean temperature variability

While positive IPO conditions may be associated with the weakening of the ENSO influence on SEA during the

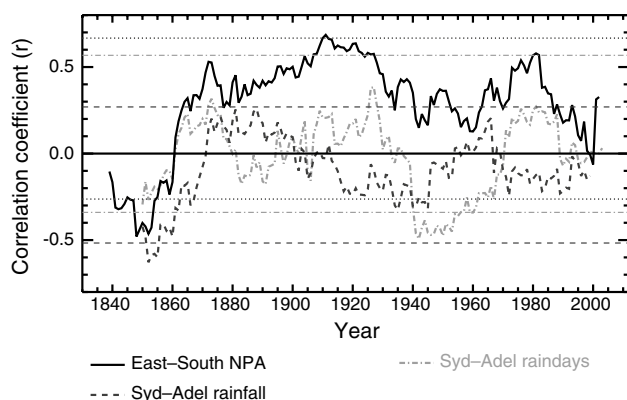


**Fig. 5** 21-year moving correlations between eastern and southern SEA rainfall, 1835–2012 (solid line), Sydney and Adelaide rainfall data, 1839–1978 (dashed black line) and Sydney and Adelaide rainday data, 1839–1978 (grey dashed line). Correlations values are plotted against the centre year of each 21-year period. Correlations values are plotted against the central year of each 21-year period. Correlations that are above or below the black dotted lines (eastern and southern NPA correlations), thin black dashed lines (Sydney and Adelaide rainfall correlations), thin grey dot-dashed lines (Sydney and Adelaide rainday correlations) are statistically significant (significance levels determined using block bootstrapping)

1830s and 1840s, low-frequency Pacific Ocean conditions do not explain the difference between eastern and southern SEA rainfall apparent during the 1830s and 1840s (Fig. 2). As mentioned in Sect. 3, prolonged wet and dry periods across the two SEA regions were largely out of phase during this time, and El Niño events during this period were in fact associated with wet conditions in southern SEA rather than the expected dry conditions.

Moving correlations between annual eastern and southern SEA rainfall, as well as rainfall and rainday totals available from 1839 to 2012 for Sydney and Adelaide are plotted in Fig. 5 to examine the long-term variability of inter-regional rainfall relationships. The 21-year moving correlations display negative values between eastern and southern SEA rainfall centred around 1850 (incorporating data from 1836 until around 1855). Strong negative correlations between Sydney and Adelaide rainfall data are also found for this period, the only time during 1839–2012. The Sydney and Adelaide rainday data correlations additionally display negative correlations during this time, although stronger negative values are observed during 1940–1960.

The negative correlation between eastern and southern SEA rainfall in the 1830s and 1840s is the most significant during the full 1832–2012 period, and is supported by analysis of the individual Sydney and Adelaide rainfall and rainday correlations. While data quality may also be playing a role here, this disagreement between the two

subregions suggests that another large-scale circulation feature dominated during this time. One possibility could be tropical Indian Ocean SSTs variations that are independent of ENSO. Although debate continues about the existence or non-existence of a dipole mode in the tropical Indian Ocean (e.g. Allan et al. 2001; Dommenges 2011; Zhao and Nigam 2015), many studies have found that SST variations in the eastern Indian Ocean at least have an impact on SEA rainfall that is independent of ENSO (e.g. Meyers et al. 2007; Ummenhofer et al. 2011; Pepler et al. 2014). Tropical Indian Ocean SSTs (generally represented by the Indian Ocean Dipole, IOD) are also known to affect eastern and southern SEA rainfall and MSLP differently (Risbey et al. 2009; Ashcroft et al. 2014b; Pepler et al. 2014).

Gergis et al.'s (2012) reconstruction of SEA rainfall identified the 1820–1840 period as a time of very wet conditions in SEA, in agreement with the 1836–1839 instrumental and documentary data from southern and inland SEA (Fig. 2; Fenby and Gergis 2013). The Gergis et al. (2012) reconstruction was developed using 12 remote proxy records that are sensitive to Indian, Southern and Pacific Ocean variability. ENSO reconstructions indicate that neutral or El Niño conditions dominated during the 1830s (e.g. Gergis and Fowler 2009; Li et al. 2013), which are generally not conducive to positive rainfall anomalies across southern SEA (Risbey et al. 2009). Therefore it could be that warm eastern Indian Ocean SSTs, or negative IOD conditions, led to the wet years being identified in the palaeoclimate and southern SEA instrumental rainfall record. Indeed negative IOD events in the absence of a strong ENSO phase are linked to wet southern SEA conditions and a dry east Australian coast (Meyers et al. 2007).

A reconstruction of SSTs in the eastern Indian Ocean (D'Arrigo et al. 2006) suggests that the 1830s and 1840s was dominated by warm SSTs, indicative of negative IOD conditions which are conducive to above-average rainfall in southern SEA. However, the 1836–1838 period stands out as a time of cold SSTs across the entire Indian Ocean, in response to a volcanic eruption in 1835 (Cole et al. 2000; D'Arrigo et al. 2006). This disagreement makes it difficult to determine the most likely IOD phase, or dominant Indian Ocean SST pattern that occurred between 1835 and 1850. Furthermore the early 1840s saw wet conditions dominating the east coast and dry years across southern SEA (Fig. 2), which is inconsistent with the rainfall signal of any IOD phase. However, without additional information on historical Indian Ocean or IOD variability it is hard to determine this dynamical change with any certainty. Further research is required to examine the impact of Indian Ocean SSTs on southern and eastern SEA rainfall during the nineteenth century.

#### 5.4 Southern Annular Mode

Another large-scale circulation feature that can cause an out-of-phase spatial relationship between southern and eastern SEA rainfall is variations in the strength and location of the midlatitude westerly winds, generally represented by the Southern Annular Mode (SAM). Reconstructions of SAM variability (Villalba et al. 2012; Abram et al. 2014) suggest that most of the 1788–1830 period was dominated by strong negative SAM conditions. In SEA, negative SAM conditions usually result in increased rainfall over southern SEA in conjunction with enhanced westerlies over the region, and decreased rainfall over the east coast due to reduced onshore precipitation (Hendon et al. 2007).

According to Abram et al. (2014)'s SAM reconstruction, 1839–1841 was a short period of relatively positive SAM conditions, favouring increased rainfall across eastern SEA and dry conditions in the south, with negative conditions present for much of 1832–1838 and 1842–1845. These SAM variations largely agree with the observed 1835–1850 SEA rainfall variability: wet conditions over southern SEA during negative SAM phases from 1836 to 1840, and wet conditions over eastern SEA when SAM was positive in the early 1840s. Villalba et al. (2012)'s reconstruction also indicates negative SAM conditions from 1830 to 1839 and during the 1840s, with relatively positive conditions only apparent in 1840–1841.

The prevalence of negative SAM conditions in the 1830s is similar to the extended negative SAM phase seen during the 1920s–1950s in both the Villalba et al. (2012) and Abram et al. (2014) reconstructions. An additional SAM reconstruction from Goodwin et al. (2004) also identified the 1900–1950 period as a time of predominantly negative SAM conditions. Figure 6 displays the 21-year moving correlations between eastern and southern SEA and ENSO again along with the 21-year moving average of the Abram et al. (2014) and Villalba et al. (2012) SAM reconstructions. Although the periods of low ENSO–SEA rainfall correlations and negative SAM conditions do not overlap exactly, there does seem to be co-occurrence of negative SAM conditions during times of weak ENSO teleconnection. This indicates that there may be some relationship between the SAM, or at least variations in the mid-latitude meridional MSLP gradient, and SEA rainfall–ENSO teleconnection variability.

Negative SAM conditions can be associated with a decrease in La Niña teleconnections across the southern Pacific region during austral summer, because the two climate modes have opposing pressure and tropospheric wind signals in the mid-southern latitudes (Karoly 1989; Fogt et al. 2010). Similarly, Fogt and Bromwich (2006) suggest that ENSO teleconnections in the western Antarctic region are weakened when ENSO is weakly or negatively

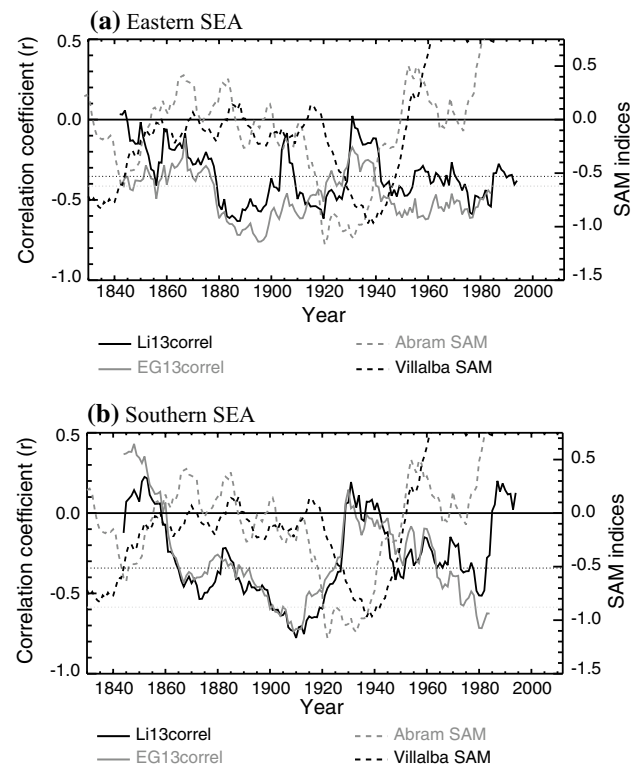


**Fig. 6** As Fig. 3 but with 21-year moving SAM variations shown, calculated from Villalba et al. (2012) and Abram et al. (2014). Both SAM reconstructions have been reset to a zero mean over the plotted period (1830–2012) for ease of comparison

correlated with SAM conditions during austral spring. Although SEA is in a different region, negative SAM conditions coupled with positive IPO conditions may have resulted in a reduction of La Niña conditions and a suppression of the influence of any La Niña event that did occur. The lack of wet years during La Niña events in the early 1800s, identified in the documentary record by Fenby and Gergis (2013) and Gergis and Ashcroft (2013) appears to support this result.

However, other SAM reconstructions identified predominantly positive SAM conditions during the 1920–1959 period. The extended instrumental SAM index of Visbeck (2009) and the tree-ring based reconstruction of Jones and Widmann (2004) both show prolonged positive SAM phases during the first half of the twentieth century. Rakich et al. (2008) additionally identified the 1940–1960 period as a time of enhanced easterly flow over eastern Australia, which is usually associated with positive SAM conditions. The Abram et al. (2014) and Villalba et al. (2012) reconstructions also display different variations during the early 1830s, and are only moderately correlated ( $r = 0.32$  over 1788–2006). Finally, the weak Li13–eastern SEA rainfall correlations in the recent period (shown in Fig. 3b) occur against a backdrop of a well known trend towards positive

SAM conditions (Arblaster and Meehl 2006). These disagreements between the SAM phases during both periods of low ENSO teleconnections must be considered when drawing conclusions about the nineteenth century ENSO teleconnection breakdown. More work into historical and palaeoclimate SAM variability as well the dynamics of SAM–ENSO interactions is needed to build on these findings.

## 6 Conclusions

The newly extended climate datasets for SEA analysed here have provided an opportunity for the first instrumental examination of the stationarity of regional teleconnections with Southern Hemisphere circulation modes for the first 225 years of European settlement in Australia. Comparing historical rainfall data to a range of palaeoclimate indices reveals that the correlations between SEA rainfall and ENSO have varied greatly since 1788. Weakened ENSO–SEA rainfall teleconnections have been identified during 1835–1850 across southern SEA in particular, supporting palaeoclimate analysis on SEA rainfall variability and in agreement with previous studies identifying a decrease in ENSO teleconnections during the first half of the nineteenth century.

There are however some important caveats that must be considered with these findings, particularly related to data distribution and quality. The geographical biases of early settlement in SEA mean that historical instrumental climate data are confined to the coastal regions until the mid-1850s, away from the inland area where rainfall is more significantly correlated with ENSO. Therefore the results obtained here cannot be extended to the wider SEA region, particularly into the interior for which historical instrumental observations are yet to be located. A lack of metadata for the historical records also creates some unavoidable uncertainty about the reliability of the data. Despite these shortcomings, the historical SEA rainfall data provide new insight into ENSO teleconnection stationarity during a time that is largely unexplored in Australian climate analysis.

Examining teleconnection variability separately over eastern and southern SEA using several datasets reveals that the majority of the variations in teleconnection strength in the early to mid-nineteenth century occurred in southern SEA rather than eastern SEA. The 1835–1850 period of low ENSO–southern SEA rainfall correlations is coincident with a combination of reduced La Niña events and ENSO variance associated with positive IPO phases, with the possible presence of a predominately negative phase of the SAM. These conditions may have caused the decrease in the correlation between SEA rainfall and ENSO, as well

as the anti-correlation between eastern and southern SEA rainfall identified during 1835–1850.

Further research is now required to identify the significance and spatial extent of the ENSO teleconnection variability over SEA during the 1800s, as well as the mechanisms behind the identified decreases in ENSO–SEA rainfall correlations. Seasonal analysis may shed more light on the interaction between ENSO, SAM and the IOD, given that each circulation feature influences each other, and SEA, at different times of the year. The use of historical reanalysis products such as future iterations of the twentieth century Reanalysis dataset (Compo et al. 2011) may assist with this and offer useful insights into atmospheric behaviour during this climatologically intriguing period. Improvements to the Southern Hemisphere palaeoclimate network and additional historical instrumental data would also provide valuable information to explain the teleconnection changes reported here. Finally, the role of global temperature changes due to volcanic eruptions or additional external drivers on the behaviour of ENSO and SAM during the mid-1800s warrants further investigation, particularly in light of the uncertainty around the influence of anthropogenic warming on future large-scale circulation behaviour.

**Acknowledgments** This study was conducted as part of the South Eastern Australian Recent Climate History (SEARCH) project, supported by the Australian Research Council (ARC) Linkage Project LP0990151. LA and DK were also supported by the ARC Centre of Excellence for Climate System Science, and JG acknowledges funding from ARC fellowship DE130100668. We thank Blair Trewin, Claire Fenby, Ailie Gallant and three anonymous reviewers for advice that helped improve this manuscript.

## References

- Abram NJ, Mulvaney R, Vimeux F, Phipps SJ, Turner J, England MH (2014) Evolution of the Southern Annular Mode during the past millennium. *Nat Clim Change* 4:564–569. doi:10.1038/nclimate2235
- Adamson GCD, Nash DJ (2014) Documentary reconstruction of monsoon rainfall variability over western India, 1781–1860. *Clim Dyn* 42:749–769
- Alexander LV, Uotila P, Nicholls N, Lynch A (2010) A new daily pressure dataset for Australia and its application to the assessment of changes in synoptic patterns during the last century. *J Clim* 23:1111–1126
- Allan RJ (2000) ENSO and climatic variability in the past 150 years. In: Diaz HF, Markgraf V (eds) *El Niño and the Southern Oscillation: multiscale variability and global and regional impacts*. Cambridge University Press, Cambridge, pp 3–35
- Allan RJ, D'Arrigo RD (1999) “Persistent” ENSO sequences: how unusual was the 1990–1995 El Niño? *The Holocene* 9:101–118. doi:10.1191/095968399669125102
- Allan RJ, Lindsay J, Parker D (1996) *El Niño: Southern oscillation and climatic variability*. CSIRO, Melbourne
- Allan RJ, Chambers D, Drosowsky W, Hendon H, Latif M, Nicholls N, Smith I, Stone RC, Tourre Y (2001) Is there an Indian Ocean

- dipole and is it independent of the El Niño–Southern Oscillation? *CLIVAR Exch* 6:18–22
- Arblaster JM, Meehl GA (2006) Contributions of external forcings to southern annular mode trends. *J Clim* 19:2896–2905. doi:[10.1175/JCLI3774.1](https://doi.org/10.1175/JCLI3774.1)
- Arblaster J, Meehl G, Moore A (2002) Interdecadal modulation of Australian rainfall. *Clim Dyn* 18:519–531. doi:[10.1007/s00382-001-0191-y](https://doi.org/10.1007/s00382-001-0191-y)
- Ashcroft L, Gergis J, Karoly DJ (2014a) A historical climate dataset for southeastern Australia, 1788–1859. *Geosci Data J* 1:158–178. doi:[10.1002/gdj.3.19](https://doi.org/10.1002/gdj.3.19)
- Ashcroft L, Karoly DJ, Gergis J (2014b) Southeastern Australian climate variability 1860–2009: a multivariate analysis. *Int J Climatol* 34:1928–1944. doi:[10.1002/joc.3639](https://doi.org/10.1002/joc.3639)
- Brázdil R, Dobrovolný P, Luterbacher J, Moberg A, Pfister C, Wheeler D, Zorita E (2010) European climate of the past 500 years: new challenges for historical climatology. *Clim Change* 101:7–40. doi:[10.1007/s10584-009-9783-z](https://doi.org/10.1007/s10584-009-9783-z)
- Cai W, van Rensch P, Cowan T (2011) Teleconnection pathways of ENSO and the IOD and the mechanisms for impacts on Australian rainfall. *J Clim* 24:3910–3923
- Cole JE, Cook ER (1998) The changing relationship between ENSO variability and moisture balance in the continental United States. *Geophys Res Lett* 25:4529–4532
- Cole JE, Dunbar RB, McClanahan TR, Muthiga NA (2000) Tropical Pacific forcing of decadal SST variability in the western Indian Ocean over the past two centuries. *Science* 287:617–619. doi:[10.1126/science.287.5453.617](https://doi.org/10.1126/science.287.5453.617)
- Compo GP, Whitaker JS, Sardeshmukh PD et al (2011) The twentieth century reanalysis project. *Q J R Meteorol Soc* 137:1–28
- D’Arrigo R, Cook E, Wilson R, Allan R, Mann ME (2005a) On the variability of ENSO over the past six centuries. *Geophys Res Lett*. doi:[10.1029/2004GL022055](https://doi.org/10.1029/2004GL022055)
- D’Arrigo R, Wilson R, Deser C, Wiles G, Cook E, Villalba R, Tudhope A, Cole J, Linsley B (2005b) Tropical-north Pacific climate linkages over the past four centuries\*. *J Clim* 18:5253–5265. doi:[10.1175/JCLI3602.1](https://doi.org/10.1175/JCLI3602.1)
- D’Arrigo R, Wilson R, Palmer JG, Krusic PJ, Curtis A, Sakulich J, Bijaksana S, Zulaikah S, Ngkoimani L, Tudhope A (2006) The reconstructed Indonesian warm pool sea surface temperatures from tree rings and corals: linkages to Asian monsoon drought and El Niño–Southern Oscillation. *Palaeoceanography* 21:PA3005–1–PA3005–13. doi:[10.1029/2005PA001256](https://doi.org/10.1029/2005PA001256)
- Dommenget D (2011) An objective analysis of the observed spatial structure of the tropical Indian Ocean SST variability. *Clim Dyn* 36:2129–2145. doi:[10.1007/s00382-101-0787-1](https://doi.org/10.1007/s00382-101-0787-1)
- Emile-Geay J, Cobb KM, Mann ME, Wittenberg AT (2013) Estimating central equatorial Pacific SST variability over the past millennium. Part II: reconstructions and implications. *J Clim* 26:2329–2352. doi:[10.1175/JCLI-D-11-00511.1](https://doi.org/10.1175/JCLI-D-11-00511.1)
- Fenby C, Gergis J (2013) A rainfall history of south-eastern Australia Part I: comparing evidence from documentary and palaeoclimate records, 1788–1860. *Int J Climatol* 33:2956–2972. doi:[10.1002/joc.3640](https://doi.org/10.1002/joc.3640)
- Fogt RL, Bromwich DH (2006) Decadal variability of the ENSO teleconnection to the high-latitude South Pacific governed by coupling with the Southern Annular Mode\*. *J Clim* 19:979–997
- Fogt RL, Bromwich DH, Hines KM (2010) Understanding the SAM influence on the South Pacific ENSO teleconnection. *Clim Dyn* 36:1555–1576. doi:[10.1007/s00382-010-0905-0](https://doi.org/10.1007/s00382-010-0905-0)
- Folland CK, Renwick JA, Salinger MJ, Mullan AB (2002) Relative influences of the interdecadal Pacific oscillation and ENSO on the South Pacific convergence zone. *Geophys Res Lett* 29:1643. doi:[10.1029/2001gl014201](https://doi.org/10.1029/2001gl014201)
- Fowler AM, Boswijk G, Lorrey AM, Gergis J, Pirie M, McCloskey SPJ, Palmer JG, Wunder J (2012) Multi-centennial tree-ring record of ENSO-related activity in New Zealand. *Nat Clim Change* 2:1–5. doi:[10.1038/nclimate1374](https://doi.org/10.1038/nclimate1374)
- Freeman GH, Halton JH (1951) Note on an exact treatment of contingency, goodness of fit and other problems of significance. *Biometrika* 38:141–149
- Gallant AJE, Phipps SJ, Karoly DJ, Muhan AB, Lorrey AM (2013) Non-stationary Australasian teleconnections and implications for paleoclimate reconstructions. *J Clim* 26:8827–8849. doi:[10.1175/JCLI-D-12-00338.1](https://doi.org/10.1175/JCLI-D-12-00338.1)
- Gergis J, Ashcroft L (2013) A rainfall history of southeastern Australia Part 2: a comparison of documentary, early instrumental and palaeoclimate records, 1788–2008. *Int J Climatol* 33:2973–2987. doi:[10.1002/joc.3639](https://doi.org/10.1002/joc.3639)
- Gergis J, Fowler A (2009) A history of El Niño–Southern Oscillation (ENSO) events since A.D. 1525: implications for future climate change. *Clim Change* 92:343–387
- Gergis J, Gallant A, Braganza K, Karoly DJ, Allen K, Cullen L, D’Arrigo R, Goodwin I, Grierson P, McGregor S (2012) On the long-term context of the 1997–2009 “Big Dry” in southeastern Australia: insights from a 206-year multi-proxy rainfall reconstruction. *Clim Change* 111:923–944. doi:[10.1007/s10584-011-0263-x](https://doi.org/10.1007/s10584-011-0263-x)
- Goodwin ID, van Ommen TD, Curran MAJ, Mayewski PA (2004) Mid latitude winter climate variability in the South Indian and southwest Pacific regions since 1300 AD. *Clim Dyn* 22:783–794. doi:[10.1007/s00382-004-0403-3](https://doi.org/10.1007/s00382-004-0403-3)
- Hendon HH, Thompson DWJ, Wheeler MC (2007) Australian rainfall and surface temperature variations associated with the Southern Hemisphere annular mode. *J Clim* 20:2452–2467. doi:[10.1175/JCLI4134.1](https://doi.org/10.1175/JCLI4134.1)
- Hendon HH, Lim E-P, Arblaster JM, Anderson DLT (2013) Causes and predictability of the record wet east Australian spring 2010. *Clim Dyn* 42:1155–1174. doi:[10.1007/s00382-013-1700-5](https://doi.org/10.1007/s00382-013-1700-5)
- Jones JM, Widmann M (2004) Atmospheric science: early peak in Antarctic oscillation index. *Nature* 432:290–291. doi:[10.1038/432290b](https://doi.org/10.1038/432290b)
- Jones DA, Wang W, Fawcett R (2009) High-quality spatial climate data-sets for Australia. *Aust Meteorol Oceanogr J* 58:233–248
- Karoly DJ (1989) Southern Hemisphere circulation features associated with El Niño–Southern Oscillation events. *J Clim* 2:1239–1252. doi:[10.1175/1520-0442\(1989\)002](https://doi.org/10.1175/1520-0442(1989)002)
- Kestin TS, Karoly DJ, Yano J-I, Rayner NA (1998) Time-frequency variability of ENSO and stochastic simulations. *J Clim* 11:2258–2272. doi:[10.1175/1520-0442](https://doi.org/10.1175/1520-0442)
- Knippertz P, Ulbrich U, Marques F, Corte-Real JO (2003) Decadal changes in the link between El Niño and springtime North Atlantic Oscillation and European–North African rainfall. *Int J Climatol* 23:1293–1311. doi:[10.1002/joc.944](https://doi.org/10.1002/joc.944)
- Lavery B, Joung G, Nicholls N (1997) An extended high-quality historical rainfall dataset for Australia. *Aust Meteorol Mag* 46:27–38
- Li J, Xie S-P, Cook ER et al (2013) El Niño modulations over the past seven centuries. *Nat Clim Change* 3:822–826. doi:[10.1038/nclimate1936](https://doi.org/10.1038/nclimate1936)
- Linsley BK, Zhang P, Kaplan A, Howe SS, Wellington GM (2008) Interdecadal–decadal climate variability from multicoral oxygen isotope records in the South Pacific Convergence Zone region since 1650 A.D. *Palaeoceanography* 23:PA2219. doi:[10.1029/2007PA001539](https://doi.org/10.1029/2007PA001539)
- Mann M, Bradley R, Hughes M (2000) Long-term variability in the El Niño/Southern Oscillation and associated teleconnections. In: Diaz HAMV, Markgraf VADH (eds) *El Niño and the Southern Oscillation: multiscale variability and global and regional impacts*. Cambridge University Press, Cambridge, pp 327–372
- McBride J, Nicholls N (1983) Seasonal relationships between Australian rainfall and the Southern Oscillation. *Mon Weather Rev* 111:1998–2004

- McGregor S, Timmermann A, Timm O (2010) A unified proxy for ENSO and PDO variability since 1650. *Clim Past* 6:1–17
- Meinke H, deVoil P, Hammer GL, Power S, Allan R, Stone RC, Folland C, Potgieter A (2005) Rainfall variability at decadal and longer time scales: signal or noise? *J Clim* 18:89–96. doi:10.1175/JCLI-3263.1
- Meyers G, McIntosh P, Pigot L, Pook M (2007) The years of El Niño, La Niña, and interactions with the tropical Indian Ocean. *J Clim* 20:2872–2880. doi:10.1175/JCLI4152.1
- Murphy B, Timbal B (2008) A review of recent climate variability and climate change in southeastern Australia. *Int J Climatol* 28:859–879
- Nash DJ, Endfield GH (2002) A 19th century climate chronology for the Kalahari region of central southern Africa derived from missionary correspondence. *Int J Climatol* 22:821–841. doi:10.1002/joc.753
- Nash DJ, Endfield GH (2008) “Splendid rains have fallen”: links between El Niño and rainfall variability in the Kalahari, 1840–1900. *Clim Change* 86:257–290. doi:10.1007/s10584-007-9274-z
- Nash D, Grab S (2010) “A sky of brass and burning winds”: documentary evidence of rainfall variability in the Kingdom of Lesotho, Southern Africa, 1824–1900. *Clim Change* 101:617–653. doi:10.1007/s10584-009-9707-y
- Nicholls N (2010) Local and remote causes of the southern Australian autumn–winter rainfall decline, 1958–2007. *Clim Dyn* 34:835–845. doi:10.1007/s00382-009-0527-6
- Nicholls N, Collins D, Trewin B, Hope P (2006) Historical instrumental climate data for Australia—quality and utility for palaeoclimatic studies. *J Quat Sci* 21:681–688
- Pepler A, Timbal B, Rakich C, Coutts-Smith A (2014) Indian Ocean Dipole overrides ENSO’s influence on cool season rainfall across the Eastern Seaboard of Australia. *J Clim* 27:3816–3826. doi:10.1175/JCLI-D-13-00554.1
- Power S, Tseitkin F, Torok SJ, Lavery B, Dahni R, McAveny B (1998) Australian temperature, Australian rainfall and the Southern Oscillation, 1910–1992: coherent variability and recent changes. *Aust Meteorol Mag* 47:85–101
- Power S, Casey T, Folland C, Colman A (1999) Inter-decadal modulation of the impact of ENSO on Australia. *Clim Dyn* 15:319–324
- Power S, Haylock M, Colman R, Wang XD (2006) The predictability of interdecadal changes in ENSO activity and ENSO teleconnections. *J Clim* 19:4755–4771. doi:10.1175/jcli3868.1
- Rakich C, Holbrook N, Timbal B (2008) A pressure gradient metric capturing planetary-scale influences on eastern Australian rainfall. *Geophys Res Lett* 35:L08713. doi:10.1029/2007GL032970
- Reason CJC, Allan RJ, Lindesay JA (1998) Climate variability on decadal time scales: mechanisms and implications for climate change. *Palaeoclimates* 3:25–49
- Risbey JS, Pook MJ, McIntosh PC, Wheeler MC, Hendon HH (2009) On the remote drivers of rainfall variability in Australia. *Mon Weather Rev* 137:3233–3253
- Ropelewski CF, Halpert MS (1987) Global and regional scale precipitation patterns associated with the El-Niño/southern oscillation. *Mon Weather Rev* 115:1606–1626
- Speer MS, Leslie LM, Fierro AO (2010) Australian east coast rainfall decline related to large scale climate drivers. *Clim Dyn* 36:1419–1429. doi:10.1007/s00382-009-0726-1
- Thiessen AH (1911) Precipitation averages for large areas. *Mon Weather Rev* 39:1082–1089. doi:10.1175/1520-0493
- Timbal B (2010) The climate of the Eastern Seaboard of Australia: a challenging entity now and for future projections. *IOP Conf Ser Earth Environ Sci* 11:012013. doi:10.1088/1755-1315/11/1/012013
- Timbal B, Drosowsky W (2013) The relationship between the decline of Southeastern Australian rainfall and the strengthening of the subtropical ridge. *Int J Climatol* 33:1021–1034. doi:10.1002/joc.3492
- Timbal B, Fawcett R (2012) A historical perspective on south-eastern Australia rainfall since 1865 using the instrumental record. *J Clim* 26:1112–1129. doi:10.1175/JCLI-D-12-00082.1
- Torrence C, Webster PJ (1999) Interdecadal changes in the ENSO–monsoon system. *J Clim* 12:2679–2690
- Trewin B, Fawcett R (2009) Reconstructing historical rainfall averages for the Murray–Darling Basin. *Bull Aust Meteorol Oceanogr Soc* 22:158–164
- Ummenhofer CC, England MH, McIntosh PC, Meyers GA, Pook MJ, Risbey JS, Gupta AS, Taschetto AS (2009) What causes southeast Australia’s worst droughts? *Geophys Res Lett* 36:L04706
- Ummenhofer CC, Gupta AS, Briggs PR, England MH, McIntosh PC, Meyers GA, Pook MJ, Raupach MR, Risbey JS (2011) Indian and Pacific Ocean influences on southeast Australian drought and soil moisture. *J Clim*. doi:10.1175/2010JCLI3475.1
- van Oldenborgh GJ, Burgers G (2005) Searching for decadal variations in ENSO precipitation teleconnections. *Geophys Res Lett* 32:L15701. doi:10.1029/2005GL023110
- Verdon DC, Franks SW (2006) Long-term behaviour of ENSO: interactions with the PDO over the past 400 years inferred from paleoclimate records. *Geophys Res Lett* 33:L06712. doi:10.1029/2005GL025052
- Verdon-Kidd DC, Kiem AS (2009) Nature and causes of protracted droughts in southeast Australia: comparison between the Federation, WWII, and Big Dry droughts. *Geophys Res Lett*. doi:10.1029/2009GL041067
- Villalba R, Lara A, Masiokas MH et al (2012) Unusual Southern Hemisphere tree growth patterns induced by changes in the Southern Annular Mode. *Nat Geosci* 5:793–798. doi:10.1038/ngeo1613
- Visbeck M (2009) A station-based Southern Annular Mode Index from 1884 to 2005. *J Clim* 22:940–950. doi:10.1175/2008JCLI2260.1
- Wittenberg AT (2009) Are historical records sufficient to constrain ENSO simulations? *Geophys Res Lett*. doi:10.1029/2009GL038710
- Lough J (2007) Tropical river flow and rainfall reconstructions from coral luminescence: Great Barrier Reef, Australia. *Paleoceanography* 22:PA2218. doi:10.1029/2006PA001377
- Zhao Y, Nigam S (2015) The Indian Ocean dipole: a monopole in SST. *J Clim* 28:3–19. doi:10.1175/JCLI-D-14-00047.1
- Zwiers FW, Zhang X, Feng Y (2011) Anthropogenic influence on long return period daily temperature extremes at regional scales. *J Clim* 24:881–892. doi:10.1175/2010JCLI3908.1